Dengqiu Ma ✉
Yongping Liu
Zhenhuan Ye
Dawei Li
Yang Wu

https://doi.org/10.21278/TOF.474044222
ISSN 1333-1124
eISSN 1849-1391

INFLUENCE OF CUTTER ERRORS ON FORMING ACCURATE VARIABLE HYPERBOLIC CIRCULAR ARC TOOTH TRACE CYLINDRICAL GEARS

Summary

The cutter error is an important factor in the accurate forming of the variable hyperbolic circular arc tooth trace (VH-CATT) cylindrical gears. Also, the study of the relationship between the cutter error and the forming of accurate teeth is beneficial for the gear modification design and the improvement in contact performance. Firstly, based on the principle of forming VH-CATT cylindrical gears, the sources of error in the tooth forming related to accuracy were analysed, including the errors in the cutter position and the cutter geometry, such as the error of rotation around the x-axis γ, the error of rotation around the y-axis β, the error of translation along the x-axis Δx, the error of translation along the y-axis Δy, the error of translation along the z-axis Δz, the pressure angle error $\Delta\alpha$ and the tooth line radius error ΔR_{T}. Next, based on the meshing theory and processing, an ideal tooth surface equation and a tooth surface equation with cutter errors were derived, and the tooth surface reconstruction was done. Then, the gear tooth thickness error was defined to characterize the accuracy of gear forming. Finally, the influences of the cutter error on the tooth thickness error and gear contact were investigated. The study shows that all cutter errors have certain influence on the tooth thickness error, contact area and load distribution; Δx has basically no effect on the gear tooth thickness error; Δx and γ make the actual meshing point deviate from the middle section. The study content and the applied methods are helpful in the tooth surface error traceability, the counter-adjustment of the tooth surface processing and the modification design. This study provides also a basis for gear design and load-bearing contact analysis.

Key words: *cutter error, variable hyperbolic circular arc tooth trace cylindrical gear, forming accuracy, tooth surface equation, tooth thickness error*

1. Introduction

To overcome the shortcomings of the traditional gear, the circular arc gear has been developed. Then, the gear tooth profile was developed as circular arc tooth profile, the middle section tooth profile as involute, and the other section tooth profiles as variable hyperbolic family, which is called the variable hyperbolic circular arc tooth trace (VH-CATT) cylindrical

gear. The gear has the advantages of spur gears, bevel gears and herringbone gears, and has a good application prospect in the field of high speed and heavy-duty transmission [1-3].

At present, the VH-CATT cylindrical gear has achieved positive results related to the meshing principle, 3D model and contact performance, manufacturing and product application. For example, Tseng J. T. [4-5], Zhao Fei [6] and Song Aiping [7] devised a space coordinate system to deduce the meshing function, meshing equation, tooth surface equation, contact line equation, curvature formula, lubrication angle formula, etc. Ma et al. [8-9] proposed a double-sided generation method to process the circular arc gear, achieved a CNC process for modifying the gear tooth surface and analysed the real tooth surface contact problem. Hou Li completed a gear parametric model based on UG, but the model was not accurate [10], hence, he made an accurate gear 3D model based on the mathematical model by using MATLAB [6]. Ma Dengqiu [11-12] developed a meshing contact impact model to analyse the characteristics of the meshing contact impact of the VH-CATT cylindrical gear, such as the impact of the stress distribution law on the tooth surface. Sun Zhijun [13] and Wei Yongqiao [14] developed a contact stress calculation model of the VH-CATT cylindrical gear based on the Hertz contact theory, which provided a reference for the calculation of the contact stress of the gear. Many other researchers also investigated contact strength, bending strength, gear transmission errors, computerized design and simulation of meshing [15-19], including a comparison of the maximum contact stress in spur gears, helical gears and VH-CATT cylindrical gears, applying the finite element analysis as the research method.

According to current literature, the research on the forming of accurate VH-CATT cylindrical gears is not in-depth. However, the geometric characteristics of VH-CATT cylindrical gears are complex. When the cutter has errors, it will further aggravate the complexity of the tooth surface geometric characteristics, and then affect the dynamic contact characteristics of the gear. Therefore, it is important to study the relationship between the cutter error and the forming of accurate gears to facilitate the design, processing and application of VH-CATT cylindrical gears.

As regards the tooth surface error, Gosselin [20] analysed the influence of adjustment parameter errors in a machine tool on the transmission performance of the spiral bevel gear. Litivn [21] analysed the influence of the machine tool error on the gear tooth surface contact position and transmission performance. Tang Jinyuan [22] proposed a contact analysis method for the spiral bevel gear transmission with errors based on the error modelling theory of a multi-body system and the gear meshing principle. The study shows that the motion error and the installation error of the machine tool have a great impact on the gear contact quality. Tang Jinyuan also derived an analytical expression of the normal error at any position of the tooth surface considering the machine tool adjustment parameter errors based on the meshing principle, and proposed a concept of the error influence coefficient [23]. Zhou Chao [24] studied the influence of the eccentricity error and the error of perpendicularity in the grinding wheel spindle on the tooth surface error of the spiral bevel gear, and proposed a concept of the sensitive direction error and a calculation method for determining the sensitive direction error. The study provides a basis for the research on the relationship between the cutter error and the geometric properties of VH-CATT cylindrical gears.

In the present paper, the sources of error related to tooth forming accuracy were analysed, such as the cutter position error and the cutter geometry error. Based on the meshing theory and processing, using the space meshing theory and differential geometry, an ideal tooth surface equation and a tooth surface equation with cutter errors were deduced. Because tooth thickness is one of the important tooth profile features, the tooth thickness error of the gear is used to characterize the accuracy of gear forming. Finally, the influences of the cutter errors on the tooth thickness error and gear contact were investigated. The research results provide a reference for the design, profile modification and lubrication of VH-CATT cylindrical gears.

2. Principle of forming and analysis of source of error in the gear tooth surface forming

VH-CATT cylindrical gears are processed by double-edged rotary milling with a large cutter head shown in Fig. 1. The rotary knife dish is mounted on the spindle of a special machine tool used for forming VH-CATT cylindrical gears and revolves around it with the angular velocity ω_d. The distance between the cutter axis and the machine spindle axis is R_T, namely the tool radius, which can also be called the tooth line radius. In the case of the VH-CATT cylindrical gear, one of the main structural parameters of the gear teeth is the tooth line radius, so, henceforth R_T is used to represent the tooth line radius The workpiece rotates around its own axis during machining with the angular velocity ω_1, it forms a close generating motion with the reciprocating motion v_t of the blade along the x-axis. When the tooth is cut completely, the workpiece rotates to the next position for cutting until the whole gear is cut. This processing method can cut the concave and the convex tooth surface at the same time, and it can ensure the accuracy of machining the tooth shape as well as processing efficiency.

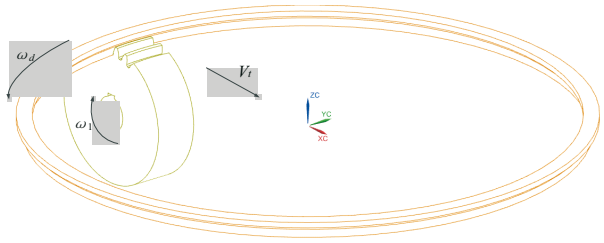

Fig. 1 Forming principle of VH-CATT cylindrical gear

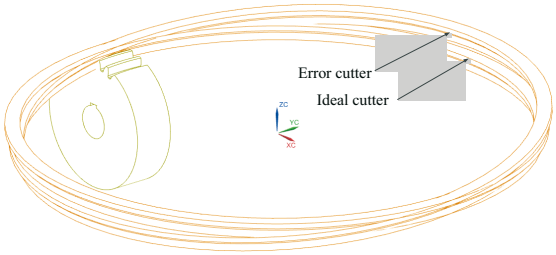

Fig. 2 Position error of VH-CATT cylindrical gear

In the actual machining, the parts of a special machine tool used for manufacturing VH-CATT cylindrical gears are affected by manufacturing error, installation error as well as deformation and abrasion. The contact position between the cutter blade and the workpiece will deviate from an ideal position. That is to say, there are errors in the machining of VH-CATT cylindrical gears. It is very complicated to directly develop a model incorporating the installation and manufacturing errors, working conditions, wear and deformation. Direct modelling is not conducive to adequate gear design and processing. However, in the case of any source of error, the tooth profile error is caused by the cutter position or blade geometry error. Therefore, it is only necessary to study the influence of the cutter position error and the geometric error on the accuracy of forming VH-CATT cylindrical gears. Fig. 2 shows a schematic diagram of the cutter position error, and Fig. 3 shows a schematic diagram of the cutter geometry error.

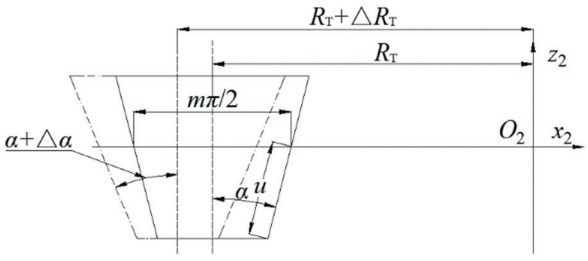

Fig. 3 Cutter geometry error of VH-CATT cylindrical gear

Theoretically, the cutter head has six position errors, including three rotation errors and three translation errors. γ, β and δ are errors of rotation around the x-, y- and z-axis, respectively. Δx, Δy and Δz are errors of translation along the x-, y- and z-axis, respectively. δ has no effect on the gear forming accuracy theoretically. In addition, the cutter has two cutter geometry errors, namely the pressure angle error $\Delta\alpha$ and the tooth line radius error ΔR_T. Therefore, this paper studies the influence of γ, β, Δx, Δy, Δz, $\Delta\alpha$ and ΔR_T on the accuracy of forming VH-CATT cylindrical gears.

3. Tooth surface equation of VH-CATT cylindrical gear

3.1 Ideal gear tooth surface equation

The reference coordinate system of an ideal CATT cylindrical gear was set up as shown in Fig. 4. Fig. 4 (*b*) is the extracted coordinate transformation system. $O_1X_1Y_1Z_1$ is the dynamic coordinate system for the gear blank; $O_2X_2Y_2Z_2$ is the dynamic coordinate system for the cutter; $O_3X_3Y_3Z_3$ is the static coordinate systems for the cutter; $O_fX_fY_fZ_f$ is the static coordinate systems for the gear blank; $O_0X_0Y_0Z_0$ is the auxiliary coordinate system. R_1 is the pitch circle of the gear blank; m is the gear module; B is the gear face width of the gear blank; ω is the rotational speed of the cutter head; ω_1 is the rotational speed of the gear blank; θ is the cutter head angle; φ_1 is the rotation angle of the gear blank.

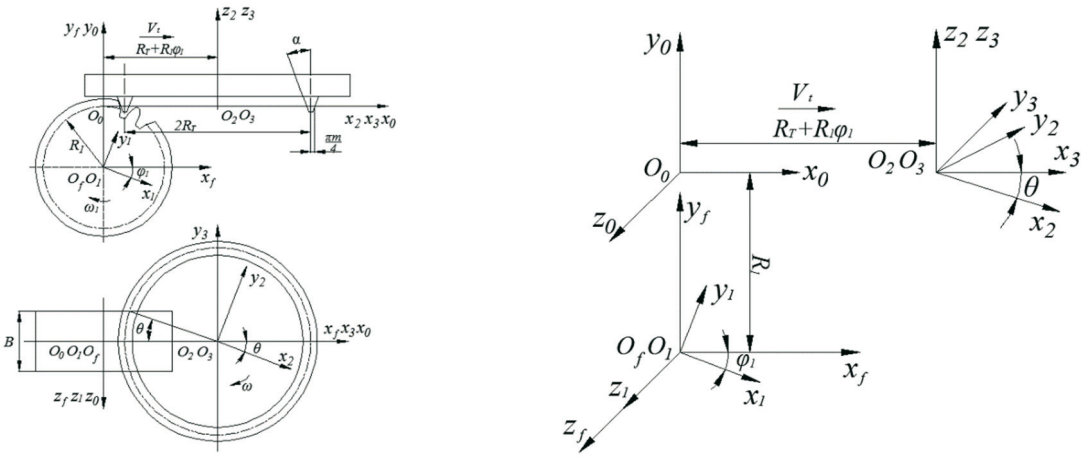

(*a*) machining coordinate system (*b*) coordinate transformation system

Fig. 4 Reference coordinate system of ideal VH-CATT cylindrical gear

According to the tool profile shown in Fig. 3, the cutter equation in $O_2X_2Y_2Z_2$ could be written as:

$$\boldsymbol{r}_2^d = -\left(R_{\mathrm{T}} \pm \frac{\pi}{4}m \pm u\sin\alpha\right)\boldsymbol{i}_2 + u\cos\alpha\boldsymbol{k}_2, \tag{1}$$

where α is the pressure angle of the cutter, u is the displacement from a random point on the cutting tool surface to a reference point in the direction of the cutting edge; '$\pm$' represents the tool cutting edge outside and inside, respectively.

By applying coordinate transformation, the cutter equation in $O_3X_3Y_3Z_3$ could be written as:

$$\boldsymbol{r}_3^d = -\left(R_{\mathrm{T}} \pm \frac{\pi}{4}m \pm u\sin\alpha\right)\cos\theta\boldsymbol{i}_3 + \left(R_{\mathrm{T}} \pm \frac{\pi}{4}m \pm u\sin\alpha\right)\sin\theta\boldsymbol{j}_3 + u\cos\alpha\boldsymbol{k}_3. \tag{2}$$

According to the meshing principle [25], the position vectors of the gear blank and the cutter are the same at the contact point, and the relative speed $\boldsymbol{v}_3^{dg}$ between the gear blank and the cutter at the contact point is perpendicular to the common normal vector $\boldsymbol{n}_3^d$ at the contact point, namely,

$$\boldsymbol{n}_3^d \cdot \boldsymbol{v}_3^{dg} = 0, \tag{3}$$

where

$$\boldsymbol{n}_3^d = \frac{\partial \boldsymbol{r}_3^d}{\partial \theta} \times \frac{\partial \boldsymbol{r}_3^d}{\partial u} \tag{4}$$

$$\boldsymbol{v}_3^{dg} = \left(\boldsymbol{\omega}_3^d \times \boldsymbol{r}_3^d + \boldsymbol{v}_d\right) - \left(\boldsymbol{\omega}_3^g \times \boldsymbol{r}_3^d + \boldsymbol{E}_3 \times \boldsymbol{\omega}_3^g\right), \tag{5}$$

where $\boldsymbol{v}_3^d$ is the cutter speed; $\boldsymbol{v}_3^g$ is the gear blank speed; $\boldsymbol{\omega}_3^d$ is the rotational angular speed of the cutter; $\boldsymbol{v}_d$ is the translation speed of the cutter; $\boldsymbol{\omega}_3^{\mathrm{g}}$ is the rotational angular speed of the gear blank; $\boldsymbol{E}_3$ is the expression of O_3 to O_1. All parameters are expressions of the contact point in the coordinate system $O_3X_3Y_3Z_3$.

According to the spatial geometric position of the coordinate systems $O_1X_1Y_1Z_1$, $O_fX_fY_fZ_f$ and $O_3X_3Y_3Z_3$, there is a relationship shown as Eq. (6).

$$\boldsymbol{k}_1 = \boldsymbol{k}_f = -\boldsymbol{j}_3 \tag{6}$$

Namely, $\boldsymbol{E}_3$, $\boldsymbol{\omega}_3^d$, $\boldsymbol{\omega}_3^{\mathrm{g}}$ and $\boldsymbol{v}_d$ could be written as:

$$\boldsymbol{E}_3 = -\left(R_{\mathrm{T}} + R_1\varphi_1\right)\boldsymbol{i}_3 - R_1\boldsymbol{k}_3 \tag{7}$$

$$\boldsymbol{\omega}_3^d = 0 \tag{8}$$

$$\boldsymbol{\omega}_3^g = \omega_1\boldsymbol{j}_3 \tag{9}$$

$$\boldsymbol{v}_d = \omega_1 R_1\boldsymbol{i}_3 \tag{10}$$

According to the gear geometry, the expression of the contact point between the cutter and the gear blank in the coordinate system $O_1X_1Y_1Z_1$ is the ideal tooth surface equation. By the coordinate transformation from $O_3X_3Y_3Z_3$ to $O_1X_1Y_1Z_1$, the ideal tooth surface equation can be expressed as:

$$\boldsymbol{r}_1^g = \boldsymbol{M}_{13}\boldsymbol{r}_3^d \tag{11}$$

and

$$\boldsymbol{M}_{13} = \boldsymbol{M}_{1f}\boldsymbol{M}_{f0}\boldsymbol{M}_{03} = \begin{bmatrix} \cos\varphi_1 & 0 & -\sin\varphi_1 & \left(R_{\mathrm{T}} + R_1\varphi_1\right)\cos\varphi_1 - R_1\sin\varphi_1 \\ \sin\varphi_1 & 0 & \cos\varphi_1 & \left(R_{\mathrm{T}} + R_1\varphi_1\right)\sin\varphi_1 + R_1\cos\varphi_1 \\ 0 & -1 & 0 & 0 \\ 0 & 0 & 0 & 0 \end{bmatrix}, \tag{12}$$

where $\boldsymbol{M}_{1f}$ is the coordinate transformation matrix from $O_fX_fY_fZ_f$ to $O_1X_1Y_1Z_1$; $\boldsymbol{M}_{f0}$ is the coordinate transformation matrix from $O_fX_fY_fZ_f$ to $O_0X_0Y_0Z_0$; $\boldsymbol{M}_{03}$ is the coordinate transformation matrix from $O_0X_0Y_0Z_0$ to $O_3X_3Y_3Z_3$.

Combining Eqs. (2), (3), (4), (5), (6), (7), (8), (9), (10) and (11), the ideal tooth surface equation of the VH-CATT cylindrical gear can be expressed as:

$$\begin{cases} x_1 = \left[-\left(R_{\mathrm{T}} \pm \dfrac{\pi}{4}m \pm u\sin\alpha\right)\cos\theta + \left(R_T + R_1\varphi_1\right)\right]\cos\varphi_1 - (R_1 + u\cos\alpha)\sin\varphi_1 \\ y_1 = \left[-\left(R_{\mathrm{T}} \pm \dfrac{\pi}{4}m \pm u\sin\alpha\right)\cos\theta + \left(R_T + R_1\varphi_1\right)\right]\sin\varphi_1 + (R_1 + u\cos\alpha)\cos\varphi_1 \\ z_1 = -\left(R_{\mathrm{T}} \pm \dfrac{\pi}{4}m \pm u\sin\alpha\right)\sin\theta \\ u = \mp\dfrac{\sin\alpha}{\cos\theta}\left[\cos\theta\left(R_T \pm \dfrac{\pi m}{4}\right) - (R_T + R_1\varphi_1)\right] \end{cases} \tag{13}$$

3.2 Tooth surface equation with cutter errors

The reference coordinate system of the tooth surface equation with cutter errors was set up as shown in Fig. 5. $O_1X_1Y_1Z_1$, $O_fX_fY_fZ_f$, $O_0X_0Y_0Z_0$, $O_2X_2Y_2Z_2$ and $O_3X_3Y_3Z_3$ are consistent with Fig. 4. $O_6X_6Y_6Z_6$ is the static coordinate system of the cutter theoretical position; $O_4X_4Y_4Z_4$ is the coordinate system with the error of rotation around the x-axis; $O_5X_5Y_5Z_5$ is the coordinate system with the error of rotation around the y-axis.

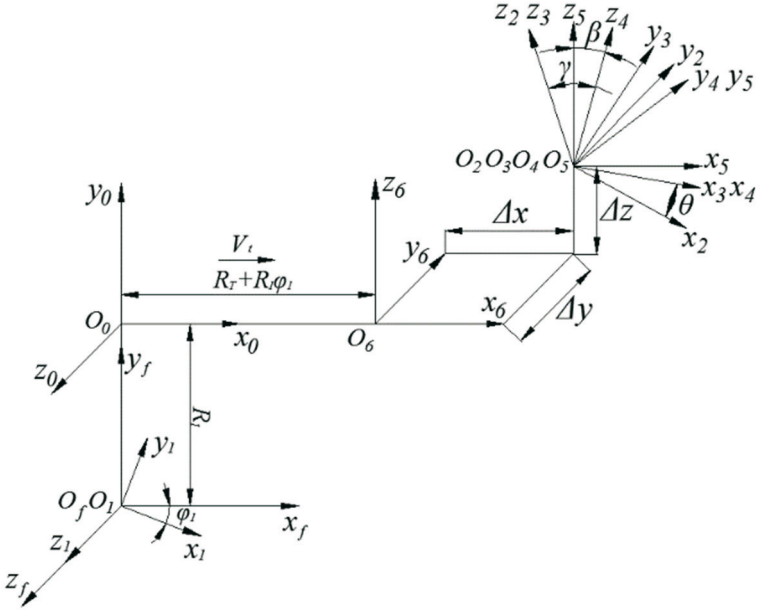

Fig. 5 Coordinate transformation system of tooth surface equation with cutter errors

3.2.1 Tool surface and normal vector with errors

According to the tool profile shown in Fig. 3, the cutter equation with errors in the $O_2X_2Y_2Z_2$ coordinate system could be written as:

$$ {}^{e}\boldsymbol{r}_2^{\,d} = -\left({}^{e}R_T \pm \frac{m\pi}{4} \pm u\sin {}^{e}\alpha \right)\boldsymbol{i}_2 + u\cos {}^{e}\alpha \boldsymbol{k}_2 , \tag{14} $$

where ${}^{e}R_T$ is the tooth line radius with errors, and ${}^{e}R_T = R_T + \Delta R_T$; ${}^{e}\alpha$ is the pressure angle of the cutter with errors, and ${}^{e}\alpha = \alpha + \Delta\alpha$; u and $\pm$ are consistent with Eq. (1).

The cutter equation with errors in $O_3X_3Y_3Z_3$ could be written as:

$$ {}^{e}\boldsymbol{r}_3^{\,d} = -\left({}^{e}R_T \pm \frac{m\pi}{4} \pm u\sin {}^{e}\alpha \right)\cos\theta \boldsymbol{i}_3 + \left({}^{e}R_T \pm \frac{m\pi}{4} \pm u\sin {}^{e}\alpha \right)\sin\theta \boldsymbol{j}_3 + u\cos {}^{e}\alpha \boldsymbol{k}_3 \tag{15} $$

According to Eq. (15), the normal vector of the tool surface with errors is expressed as:

$$ {}^{e}\boldsymbol{n}_3 = \frac{\partial {}^{e}\boldsymbol{r}_3^{\,d}}{\partial u} \times \frac{\partial {}^{e}\boldsymbol{r}_3^{\,d}}{\partial \theta} = \left({}^{e}R_T \pm \frac{m\pi}{4} \pm u\sin {}^{e}\alpha \right)\left(-\cos {}^{e}\alpha \cos\theta \boldsymbol{i}_3 \pm \cos {}^{e}\alpha \sin\theta \boldsymbol{j}_3 \mp \sin {}^{e}\alpha \boldsymbol{k}_3 \right) \tag{16} $$

3.2.2 Relative speed at the contact point with errors

The relative speed with errors ${}^{e}\boldsymbol{v}^{dg}$ in the $O_3X_3Y_3Z_3$ coordinate system can be expressed as:

$$ {}^{e}\boldsymbol{v}^{dg} = {}^{e}\boldsymbol{v}_3^{d} - {}^{e}\boldsymbol{v}_3^{g} = \left({}^{e}\boldsymbol{\omega}_3^{d} \times {}^{e}\boldsymbol{r}_3^{d} + {}^{e}\boldsymbol{v}_d \right) - \left({}^{e}\boldsymbol{\omega}_3^{g} \times {}^{e}\boldsymbol{r}_3^{d} + {}^{e}\boldsymbol{E}_3 \times {}^{e}\boldsymbol{\omega}_3^{g} \right) \tag{17} $$

where ${}^{e}\boldsymbol{v}_3^d$ is the cutter speed with errors; ${}^{e}\boldsymbol{v}_3^g$ is the gear blank speed with errors; ${}^{e}\boldsymbol{\omega}_3^d$ is the rotational angular speed with cutter errors, and ${}^{e}\boldsymbol{\omega}_3^d = \boldsymbol{0}$; ${}^{e}\boldsymbol{v}_d$ is the translation speed with cutter errors, and ${}^{e}\boldsymbol{v}_d = \omega_1 R_1 \boldsymbol{i}_3$; ${}^{e}\boldsymbol{\omega}_3^{\mathrm{g}}$ is the rotational angular speed with cutter errors of the gear blank; ${}^{e}\boldsymbol{E}_3$ is the expression of O_3 to O_1.

The coordinate transformation matrix $\boldsymbol{M}_{53}$ from $O_3X_3Y_3Z_3$ to $O_5X_5Y_5Z_5$ can be written as:

$$\boldsymbol{M}_{53} = \begin{bmatrix} \cos\beta & \sin\beta\sin\gamma & -\sin\beta\cos\gamma & 0 \\ 0 & \cos\gamma & \sin\gamma & 0 \\ \sin\beta & -\sin\gamma\cos\beta & \cos\beta\cos\gamma & 0 \\ 0 & 0 & 0 & 1 \end{bmatrix} \tag{18}$$

The inverse matrix of $\boldsymbol{M}_{53}$ can be written as:

$$\boldsymbol{M}_{53}^{-1} = \begin{bmatrix} \cos\beta & 0 & \sin\beta & 0 \\ \sin\beta\sin\gamma & \cos\gamma & -\sin\gamma\cos\beta & 0 \\ -\sin\beta\cos\gamma & \sin\gamma & \cos\gamma\cos\beta & 0 \\ 0 & 0 & 0 & 1 \end{bmatrix} \tag{19}$$

The expression of O_3 to O_1 in the $O_5X_5Y_5Z_5$ can be written as ${}^{e}\boldsymbol{E}_5$:

$${}^{e}\boldsymbol{E}_5 = -\left(\Delta x + {}^{e}R_T + R_1\varphi_1\right)\boldsymbol{i}_5 - \Delta y\boldsymbol{j}_5 - \left(R_1 + \Delta z\right)\boldsymbol{k}_5 \tag{20}$$

Therefore,

$${}^{e}\boldsymbol{E}_3 = \boldsymbol{M}_{53}^{-1}\,{}^{e}\boldsymbol{E}_5 \tag{21}$$

Similarly, ${}^{e}\boldsymbol{\omega}_3^g$ can be calculated using Eq. (22).

$${}^{e}\boldsymbol{\omega}_3^g = \boldsymbol{M}_{53}^{-1}\,{}^{e}\boldsymbol{\omega}_5^g\ , \tag{22}$$

where ${}^{e}\boldsymbol{\omega}_5^g = \omega_1\boldsymbol{j}_5$.

Combining Eqs. (17), (21) and (22), the relative speed with errors ${}^{e}\boldsymbol{v}^{dg}$ can be calculated.

3.2.3 Tooth surface model with errors

Similarly, according to the meshing principle [23], ${}^{e}\boldsymbol{n}_3 \cdot {}^{e}\boldsymbol{v}_3^{dg} = 0$, the expression of u with errors can be expressed as ${}^{e}u$:

$$\begin{aligned} {}^{e}u = -\frac{1}{\cos\gamma\cos\theta}\Big[& -R_1\cos\theta\cos{}^{e}\alpha + B\cos\beta\cos\theta\cos{}^{e}\alpha - C\sin\beta\cos\theta\cos{}^{e}\alpha \\ & -C\sin\gamma\cos\beta\sin\theta\cos{}^{e}\alpha \mp C\cos\gamma\cos\beta\sin{}^{e}\alpha \mp B\cos\gamma\sin\beta\sin{}^{e}\alpha \\ & -B\sin\gamma\sin\beta\sin\theta\cos{}^{e}\alpha \pm \cos\gamma\cos\theta\sin{}^{e}\alpha\left({}^{e}R_T \pm \frac{m\pi}{4}\right)\Big] \end{aligned} \tag{23}$$

where $B = R_1 + \Delta z$, $C = {}^{e}R_T + R_1\varphi_1 + \Delta x$.

The coordinate transformation of the cutter equation with errors from $O_3X_3Y_3Z_3$ to $O_1X_1Y_1Z_1$ can be expressed as:

$$ {}^{e}\boldsymbol{r}_1^{g} = {}^{e}\boldsymbol{M}_{13}\,{}^{e}\boldsymbol{r}_3^{d} \tag{24} $$

and

$$ {}^{e}\boldsymbol{M}_{13} = {}^{e}\boldsymbol{M}_{1f}\,{}^{e}\boldsymbol{M}_{f0}\,{}^{e}\boldsymbol{M}_{06}\,{}^{e}\boldsymbol{M}_{65}\,{}^{e}\boldsymbol{M}_{54}\,{}^{e}\boldsymbol{M}_{43}\ , \tag{25} $$

where ${}^{e}\boldsymbol{M}_{13}$ is the coordinate transformation matrix from $O_3X_3Y_3Z_3$ to $O_1X_1Y_1Z_1$; ${}^{e}\boldsymbol{M}_{1f}$ is the coordinate transformation matrix from $O_fX_fY_fZ_f$ to $O_1X_1Y_1Z_1$; ${}^{e}\boldsymbol{M}_{f0}$ is the coordinate transformation matrix from $O_0X_0Y_0Z_0$ to $O_fX_fY_fZ_f$; ${}^{e}\boldsymbol{M}_{06}$ is the coordinate transformation matrix from $O_6X_6Y_6Z_6$ to $O_0X_0Y_0Z_0$; ${}^{e}\boldsymbol{M}_{65}$ is the coordinate transformation matrix from $O_5X_5Y_5Z_5$ to $O_6X_6Y_6Z_6$; ${}^{e}\boldsymbol{M}_{54}$ is the coordinate transformation matrix from $O_4X_4Y_4Z_4$ to $O_5X_5Y_5Z_5$; ${}^{e}\boldsymbol{M}_{43}$ is the coordinate transformation matrix from $O_3X_3Y_3Z_3$ to $O_4X_4Y_4Z_4$. The expression of ${}^{e}\boldsymbol{M}_{13}$ is given by Eq. (26).

$$ {}^{e}\boldsymbol{M}_{13} = \begin{bmatrix} \cos(\varphi_1+\beta) & \sin\gamma\sin(\varphi_1+\beta) & -\cos\gamma\sin(\varphi_1+\beta) & ({}^{e}R_T + R_1\varphi_1 + \Delta x)\cos\varphi_1 - (R_1+\Delta z)\sin\varphi_1 \\ \sin(\varphi_1+\beta) & -\sin\gamma\cos(\varphi_1+\beta) & \cos\gamma\cos(\varphi_1+\beta) & ({}^{e}R_T + R_1\varphi_1 + \Delta x)\sin\varphi_1 + (R_1+\Delta z)\cos\varphi_1 \\ 0 & -\cos\gamma & -\sin\gamma & -\Delta y \\ 0 & 0 & 0 & 1 \end{bmatrix} \tag{26} $$

Combining Eqs. (15), (24) and (26), the tooth surface equation with cutter head errors can be expressed as:

$$ \begin{cases} {}^{e}x_1 = -\left({}^{e}R_T \pm \dfrac{m\pi}{4} \pm u\sin{}^{e}\alpha\right)\cos\theta\cos(\varphi_1+\beta) + \left[\left({}^{e}R_T \pm \dfrac{m\pi}{4} \pm u\sin{}^{e}\alpha\right)\sin\theta\sin\gamma - u\cos{}^{e}\alpha\cos\gamma\right]\sin(\varphi_1+\beta) \\ \quad + ({}^{e}R_T + R_1\varphi_1 + \Delta x)\cos\varphi_1 - (R_1+\Delta z)\sin\varphi_1 \\ {}^{e}y_1 = -\left({}^{e}R_T \pm \dfrac{m\pi}{4} \pm u\sin{}^{e}\alpha\right)\cos\theta\sin(\varphi_1+\beta) + \left[u\cos{}^{e}\alpha\cos\gamma - \left({}^{e}R_T \pm \dfrac{m\pi}{4} \pm u\sin{}^{e}\alpha\right)\sin\theta\sin\gamma\right]\cos(\varphi_1+\beta) \\ \quad + ({}^{e}R_T + R_1\varphi_1 + \Delta x)\sin\varphi_1 + (R_1+\Delta z)\cos\varphi_1 \\ {}^{e}z_1 = -\left({}^{e}R_T \pm \dfrac{m\pi}{4} \pm u\sin{}^{e}\alpha\right)\sin\theta\cos\gamma - u\cos{}^{e}\alpha\sin\gamma - \Delta y \\ {}^{e}u = -\dfrac{1}{\cos\gamma\cos\theta}\Big[-R_1\cos\theta\cos{}^{e}\alpha + B\cos\beta\cos\theta\cos{}^{e}\alpha - C\sin\beta\cos\theta\cos{}^{e}\alpha - C\sin\gamma\cos\beta\sin\theta\cos{}^{e}\alpha \\ \quad - B\sin\gamma\sin\beta\sin\theta\cos{}^{e}\alpha \pm \cos\gamma\cos\theta\sin{}^{e}\alpha\left({}^{e}R_T \pm \dfrac{m\pi}{4}\right) \mp C\cos\gamma\cos\beta\sin{}^{e}\alpha \mp B\cos\gamma\sin\beta\sin{}^{e}\alpha\Big] \end{cases} \tag{27} $$

Fig. 6 shows an error and ideal tooth surface model, whereby the ideal tooth surface is shown in red, and the error tooth surface is shown in black. The parameters are as follows: $z = 29$, $B = 80$ mm, $\alpha = 20°$, $m = 8$ mm and $R_T = 500$ mm. The part cutter error parameters are as follows: $\gamma = 0.1°$, $\Delta y = 2$ mm, $\Delta R_T = 10$ mm and $\Delta\alpha = 1°$.

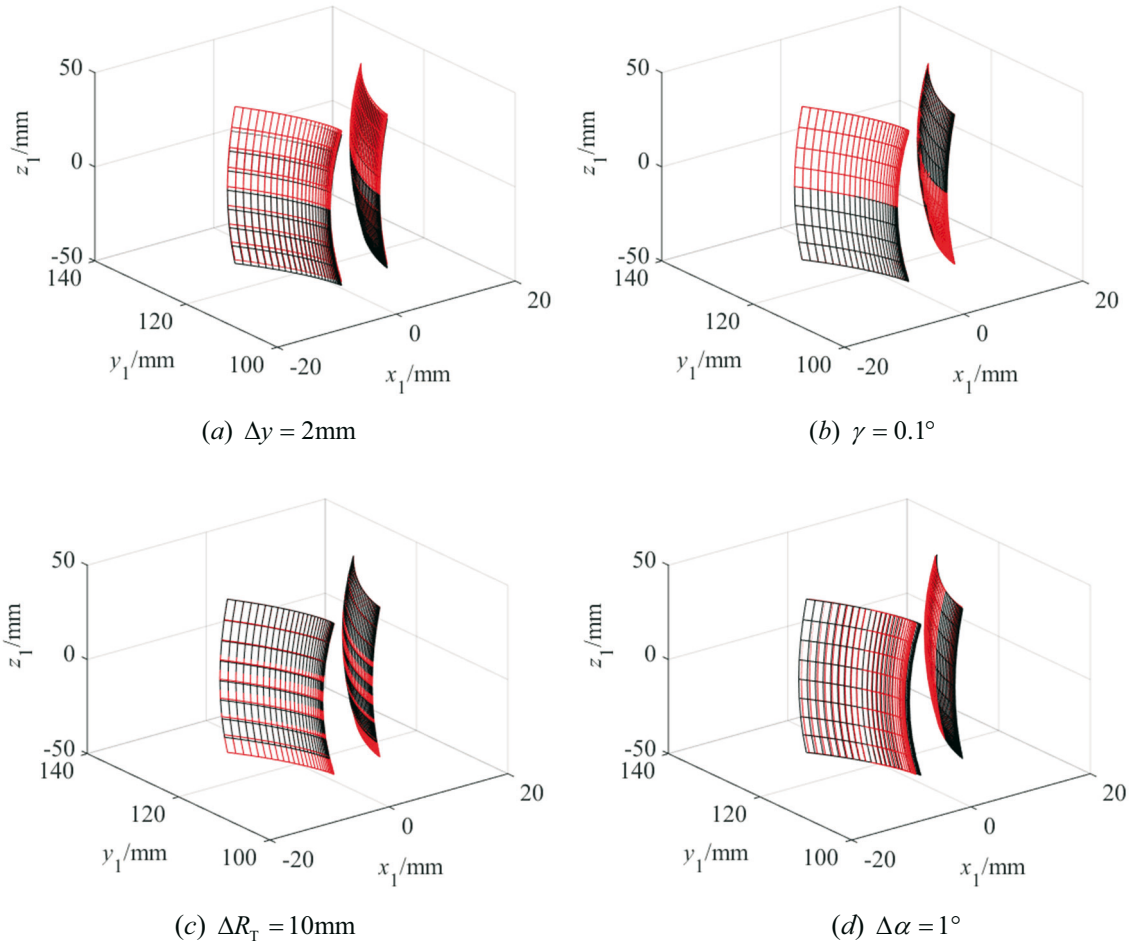

(*a*) $\Delta y = 2\text{mm}$ (*b*) $\gamma = 0.1°$

(*c*) $\Delta R_T = 10\text{mm}$ (*d*) $\Delta\alpha = 1°$

Fig. 6 Error and ideal tooth surface model

4. Tooth thickness and tooth thickness error

The tooth thickness of VH-CATT cylindrical gears is an important parameter, and it has also a great influence on the design, profile modification, lubrication, strength and measuring of gears. Therefore, the tooth thickness must be studied; especially the tooth thickness with errors must be studied. The tooth thickness of VH-CATT cylindrical gears is divided into two categories: the normal tooth thickness S_n and the circumferential tooth thickness S_t. This paper mainly discusses the circumferential tooth thickness, denoted by *S*.

The tooth thickness of an arbitrary cross section is shown schematically in Fig. 7. The arc length between point *A* and point *B* is the tooth thickness. If the coordinates of *A* and *B* are known, S_t can be calculated by Eq. (28).

$$\begin{cases} S_i = \sqrt{(A_x - B_x)^2 + (A_y - B_y)^2} \\ S = 2R_k \arcsin(\dfrac{S_i}{2R_k}) \end{cases}, \tag{28}$$

where $(x_A,\ y_A)$ are the coordinates of point *A*, (x_B, y_B) are the coordinates of point *B*, S_i is the chord length, R_k is the arbitrary circular radius between the tooth top and the base circle.

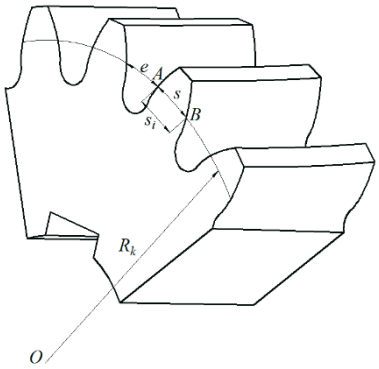

Fig. 7 Relationship between tooth thickness and chord tooth thickness

In this paper, the difference between the actual tooth thickness of VH-CATT cylindrical gears ${}^{e}S$ and the ideal tooth thickness of VH-CATT cylindrical gears S is defined as the tooth thickness error ${}^{e}S$ to characterize gear forming accuracy, expressed as Eq. (29). And the influences of β, γ, Δx, Δy, Δz, $\Delta\alpha$ and ΔR_{T} were studied.

$$S_e = {}^{e}S - S \tag{29}$$

5. Influence of cutter error on tooth thickness error

Table 1 gives basic structural parameters of VH-CATT cylindrical gears, and it is used to discuss the influence of cutter errors on the tooth thickness error, mainly including the modulus, gear number, gear face width, pressure angle and tooth line radius. The values of the structural parameters are selected by referring to literature [26].

Table 1 Main structural parameters of gears

Structural parameter	Value	Structural parameter	Value	Structural parameter	Value
Modulus m/mm	8	Pressure angle α/°	20	Gear face width B/mm	80
Gear number z	29	Tooth line radius R_{T}/mm	500		

5.1 Influence of error of rotation around y-axis β on tooth thickness error

Fig. 8 shows the influence of the error of rotation around the y-axis β on the tooth thickness error. The errors of rotation around the y-axis β are equal to 1×10^{-3} rad, 5×10^{-4} rad, -5×10^{-4} rad and -1×10^{-3} rad, respectively. β is a positive value when the error rotates clockwise around the y-axis; and β is a negative value when the error rotates counterclockwise around the y-axis.

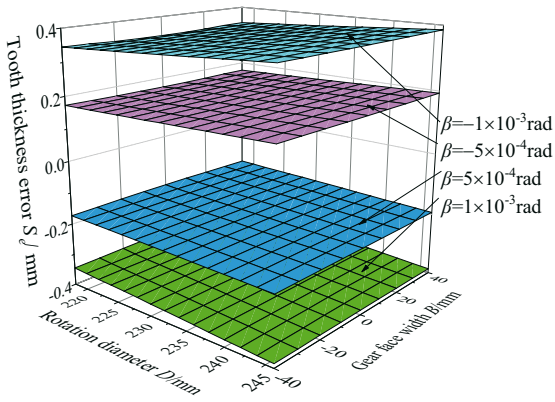

Fig. 8 Influence of β on tooth thickness error

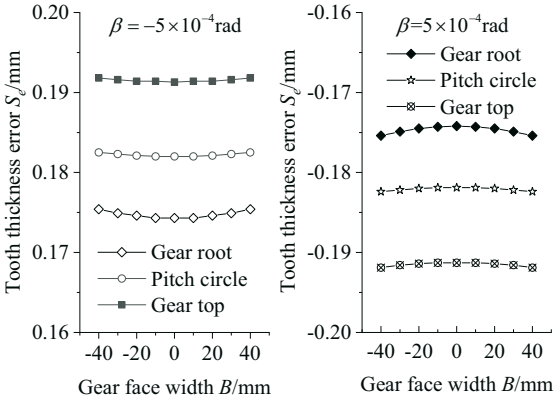

Fig. 9 Variation trend of tooth thickness error along tooth face width with β error

It is obvious that the absolute value of the tooth thickness error S_e increases with an increase in β, and the tooth thickness error is negative when the error is caused by the clockwise rotation; the tooth thickness error is positive when the error is caused by the counterclockwise rotation. It is shown that the tooth thickness decreases when the error is caused by the clockwise rotation and increases when the error is caused by the counterclockwise rotation. The reason is as follows: when the cutter rotates clockwise, it is equivalent to the tool travelling a certain distance along the direction of the z negative half axis, called negative addendum modification, the tooth thickness reduces, the tooth thickness error is negative, and the larger β is, the larger the travelling distance is, as is the tooth thickness error; when the cutter rotates counterclockwise, it is equivalent to the tool travelling a certain distance along the direction of the z positive half axis, called positive addendum modification, the tooth thickness increases, the tooth thickness error is positive, and the larger β is, the larger the travelling distance is, as is the tooth thickness error. At the same time, the absolute value of the tooth thickness error gradually increases from the gear root to the gear top in the direction of the tooth height. In addition, Fig. 9 shows that the degree of the gear drum is low when the error is caused by the counterclockwise rotation and the degree of gear drum increases when the error is caused by the clockwise rotation.

5.2 Influence of error of rotation around x-axis γ on tooth thickness error

Fig. 10 shows the influence of the error of rotation around the x-axis γ on the tooth thickness error. The errors of rotation around the x-axis γ are equal to 0.0174rad, 0.0087rad, -0.0087rad and -0.0174rad, respectively. γ is a positive value when the error rotates clockwise around the x-axis; and γ is a negative value when the error rotates counterclockwise around the x-axis.

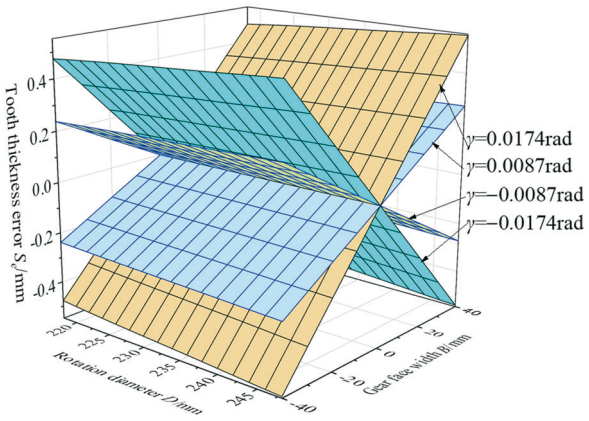

Fig. 10 Influence of γ on tooth thickness error

It is obvious that the tooth thickness error of the face width middle section is zero; the tooth thickness error of the other sections increases with an increase in γ. When the error is caused by the clockwise rotation, the tooth thickness error in the positive direction of tooth face width is positive, the tooth thickness increases, and the negative direction of the tooth face width is negative, and the tooth thickness reduces. The opposite occurs when the error is caused by the clockwise rotation. The reason is as follows: when the error is caused by the clockwise rotation, it is equivalent to the tool travelling a certain distance along the direction of the z positive half axis in the positive direction of the tooth face width, namely positive the addendum modification; in the negative direction of the tooth face width, it is equivalent to the tool travelling a certain distance along the direction of the z negative half axis, namely the negative addendum modification. The larger γ is, the larger the travelling distance is and the larger the tooth thickness error is. The reason for the counterclockwise rotation is the same as in the case of the clockwise rotation, so it is not further discussed.

5.3 Influence of error of translation along *x*-axis Δx on tooth thickness error

Fig. 11 shows the influence of the error of translation along the *x*-axis Δx on the tooth thickness error. The errors of translation along the *x*-axis Δx are equal to 2mm, 1mm, -1mm and -2mm, respectively. The translation along the direction of the *x* positive half axis has a positive value, and the translation along the direction of the *x* negative half axis has a negative value.

It is obvious that the error of translation along the *x*-axis Δx has no influence on the tooth thickness error. The reason is as follows: when the error is caused by the error of translation along the *x*-axis, a complete model of the VH-CATT cylindrical gear can be obtained by adjusting the initial position of the gear blank and the length of the cutter blade, so the tooth thickness error is basically zero. Fig. 12 shows a 3D model with no error and a model with the error Δx =2mm. It can be seen that the error 3D model is rotated by an angle β_e relative to the no error 3D model. When the error model is rotated by an angle β_e counterclockwise, the error model and the no error model coincide exactly.

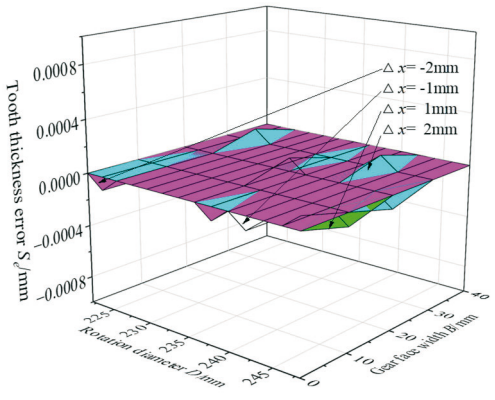

Fig. 11 Influence of Δx on tooth thickness error

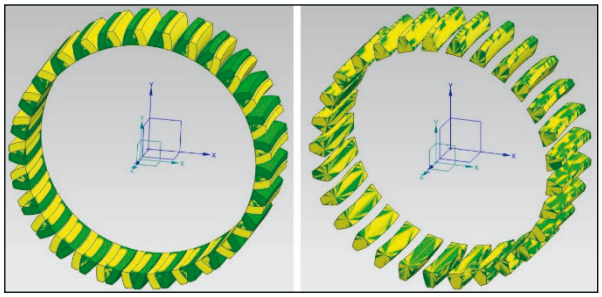

(*a*) Model before rotation (*b*) Model after rotation

Fig. 12 Error model and no error model

5.4 Influence of error of translation along *y*-axis Δy on tooth thickness error

Fig. 13 shows the influence of the error of translation along the *y*-axis Δy on the tooth thickness error. The errors of translation along the *y*-axis Δy are equal to 4mm, 2mm, -2mm and -4mm, respectively. The translation along the direction of the *y* positive half axis has a positive value, and the translation along the direction of the *y* negative half axis has a negative value.

It is obvious that the tooth thickness error increases with an increase in Δy. When the error is caused by translation along the direction of the *y* positive half axis, it is equivalent to the error occurring when the processed gear surface of the VH-CATT cylindrical gear is translated by a certain distance towards the z_1 negative half axis. So, the tooth thickness error of the z_1 negative half axis is positive, and the tooth thickness error of the z_1 positive half axis is negative. The larger Δy is, the larger the tooth thickness error is. The reason is as follows: literature [26] shows that the tooth thickness of an ideal VH-CATT cylindrical gear gradually decreases from the middle surface to the end face along the direction of the tooth face width, and the tooth is a drum-shaped tooth. When the cutter moves forward along the *y* positive half axis, the tooth thickness of the z_1 negative half axis increases, and the tooth thickness of the z_1 positive half axis decreases, then the tooth thickness error of the z_1 negative half axis is positive, and the tooth thickness error of the z_1 positive half axis is negative. The phenomenon with the error of translation along the *y* negative half axis is opposite to the error of translation along the *y* positive half axis, but the reason for the error of translation along the *y* negative half axis is the same as in the case of the error of translation along the *y* positive half axis, so it is not discussed here.

5.5 Influence of error of translation along *z*-axis Δz on tooth thickness error

Fig. 14 shows the influence of the error of translation along the *z*-axis Δz on the tooth thickness error. The errors of translation along the *z*-axis Δz are equal to 2mm, 1mm, -1mm and -2mm, respectively. The translation along the direction of the *z* positive half axis has a positive value, and the translation along the direction of the *z* negative half axis has a negative value.

It is obvious that the tooth thickness error increases with an increase in Δz. When the error is caused by translation along the direction of the z positive half axis, the tooth thickness error is positive, and when it is translated in the negative direction, the tooth thickness error is negative. The reason is as follows: when the cutter head travels a certain distance along the z positive half axis, the tooth thickness increases; when the cutter head travels a certain distance along the z negative half axis, the tooth thickness decreases. Therefore, the tooth thickness error of the positive translation is positive, and the tooth thickness error of the negative translation is negative.

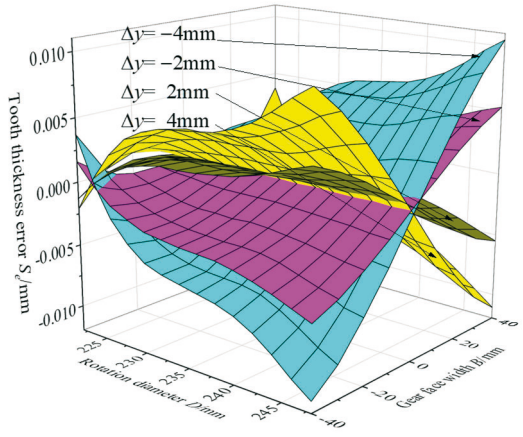

Fig. 13 Influence of Δy on tooth thickness error

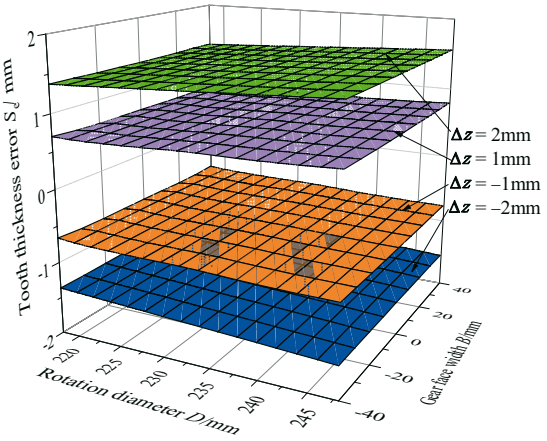

Fig. 14 Influence of Δz on tooth thickness error

5.6 Influence of pressure angle error $\Delta\alpha$ on tooth thickness error

Fig. 15 shows the influence of the pressure angle error $\Delta\alpha$ on the tooth thickness error. The pressure angle errors $\Delta\alpha$ are equal to 0.5°, 1.0°, 1.5° and 2.0°, respectively.

It is obvious that the tooth thickness error of the pitch circle is zero; the tooth thickness error from the tooth root to the pitch circle is positive, and the tooth thickness error from the pitch circle to the tooth top is negative, resulting in the tooth shape to become sharp. The reason is as follows: according to Fig. 3, the geometric dimension of the blade from the centre line to the top becomes smaller, and the geometric dimension of the blade from the centre line to the root becomes larger. Therefore, the cutting amount from the gear root to the pitch circle decreases, and the cutting amount from the pitch circle to the tooth top increases, that is, the tooth thickness near the tooth root increases, and the tooth thickness near the tooth top decreases. Therefore, the tooth thickness error of the tooth root is positive, and the tooth thickness error of the tooth top is negative.

5.7 Influence of tooth line radius error ΔR_T on tooth thickness error

Fig. 16 shows the influence of the tooth line radius error ΔR_T on the tooth thickness error. The tooth line radius errors ΔR_T are equal to 10mm, 5mm, -5mm and -10mm, respectively.

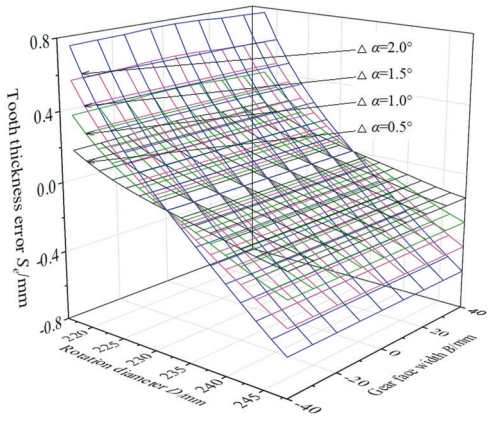

Fig. 15 Influence of $\Delta\alpha$ on tooth thickness error

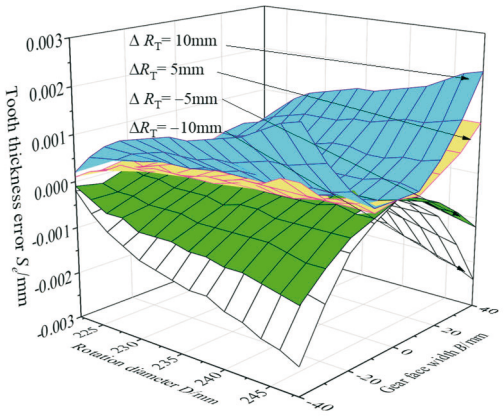

Fig. 16 Influence of ΔR_T on tooth thickness error

It is obvious that the tooth thickness error of the face width middle section is zero; when the tooth line radius error ΔR_T is greater than 0, the tooth thickness error is positive; when the tooth line radius error ΔR_T is less than 0, the tooth thickness error is negative; the larger the tooth line radius error is, the greater the absolute value of the tooth thickness error closer to the tooth top and the end face is. When ΔR_T is less than 0, the end face near the tooth top becomes sharp; when ΔR_T is greater than 0, the tooth thickness of the end face near the tooth top increases. The reason is as follows: the tooth profile from the middle section to the end face shows an intersection trend, and the tooth line radius is an important factor affecting the intersection trend. The smaller the tooth line radius is, the more obvious the intersection trend of the tooth profile is, and the more obvious the sharpening of the tooth top is. When the tooth line radius tends to infinity, the VH-CATT cylindrical gear becomes an involute spur gear, and there is no change in the tooth thickness from the middle section to the end face. In fact, the essence of the tooth line radius error is the change in the tooth line radius. When ΔR_T is less than 0, the tooth line radius decreases and the tooth top becomes sharp. When ΔR_T is greater than 0, the tooth line radius increases and the tooth thickness of the tooth top increases.

6. Influence of errors on gear contact

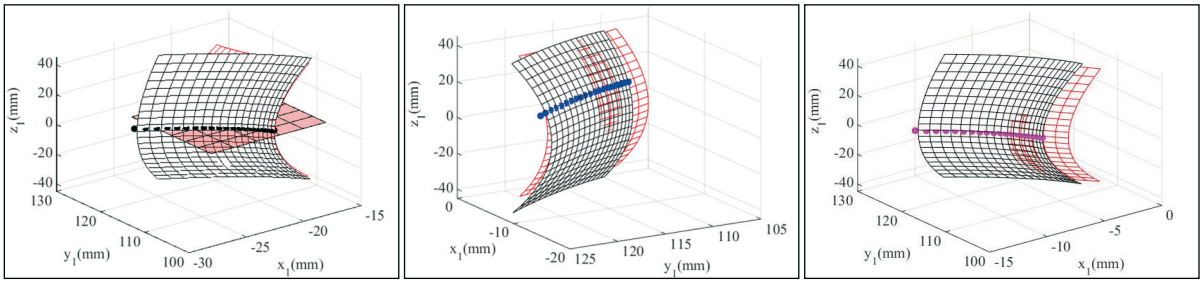

$(a)\ \gamma = 0.00174\text{rad}$ $(b)\ \Delta y = -1\text{mm}$ $(c)\ \beta = 0.00174\text{rad}$

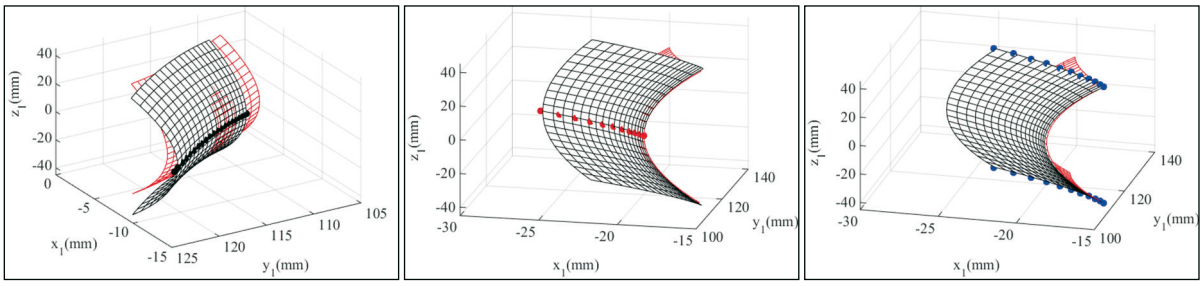

$(d)\ \Delta\alpha = 1°$ $(e)\ \Delta R_T = 5\text{mm}$ $(f)\ \Delta R_T = 20\text{mm}$

Fig. 17 Influence of cutter errors on contact position

Research shows that cutter errors have a certain influence on the tooth surface structure. It is very important to investigate the influence of cutter errors on the contact performance. The tooth contact analysis (TCA) is an effective means for analysing the gear system contact [27]. So, a TCA model was developed to calculate the actual meshing point position and the contact area, the main parameters being as follows: modulus m = 8mm, pressure angle α = 20°, gear number z_1 = 29 and z_2 = 41, tooth line radius R_T = 200mm. Fig. 17 shows the influence of the cutter errors on the contact position. The point represents the actual contact point, the black surface is the driving gear tooth surface, and the red surface is the driven gear tooth surface. It can be seen from the figure that γ and Δy make the actual meshing point deviate from the middle section, and the other error items do not change the actual meshing point position, but it does not mean that it has no effect on the contact performance. In addition, the contact point position will change to the tooth face width end face if the ΔR_T is too large, as shown in Fig. 17(*f*). Fig. 18 shows the influence of the cutter errors on the contact area of the gear pair. It indicates that all the cutter errors have an influence on the contact area, but ΔR_T and ΔR_T have a larger influence on the contact area than those of the other error items, and Δy has a larger influence on the gear top contact area than that of the gear root.

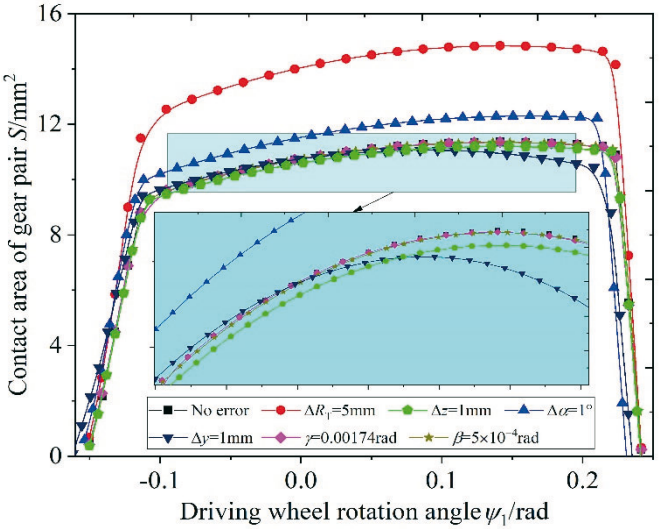

Fig. 18 Influence of cutter errors on contact area of gear pair

The load tooth contact analysis (LTCA) is an important method for analyzing the bearing situation of the tooth surface under real load. The analysis results are important technical indicators for measuring the dynamic transmission performance and they are also a link between the geometric parameter design of the tooth surface and the analysis of system dynamics behaviour [28]. Therefore, to analyse the influence of cutter errors in real contact, an LTCA model was set up and solved through mathematical programming to analyse the influence of cutter errors on the distribution of tooth surface load, Fig. 19 shows the process of the LTCA.

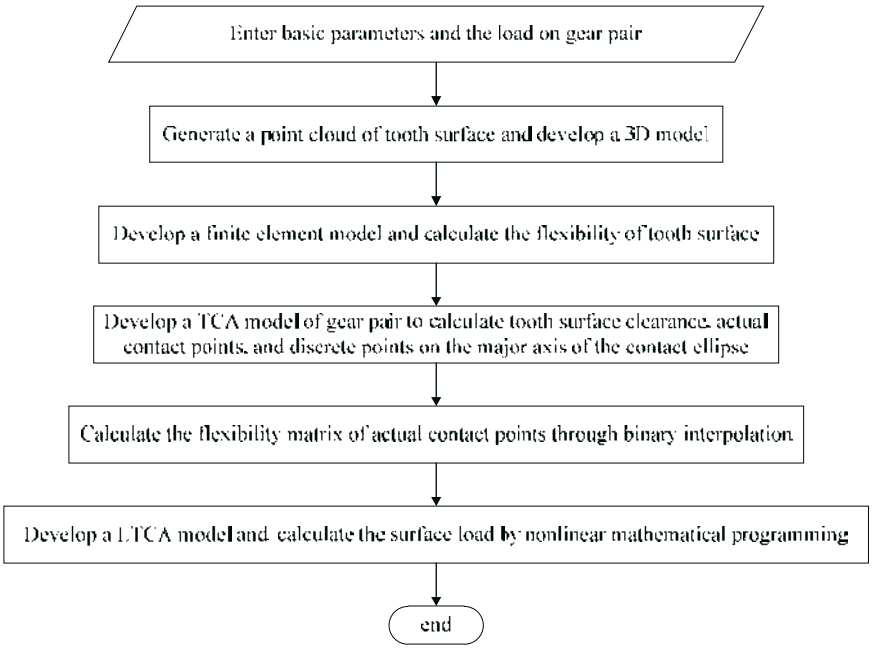

Fig. 19 LTCA process

In this paper, based on the conditions of deformation coordination, force balance, and non-embedding, the following mathematical model is developed to describe the equilibrium state of the tooth contact under load:

$$\begin{cases} f = \min\left[\dfrac{1}{2}\left(\boldsymbol{P}^T\boldsymbol{S}\right)\boldsymbol{P}\right] \\ [w]_m = -[S]_m[F]_m + s_z[e] + [d]_m, m = \mathrm{I},\mathrm{II} \\ T = \sum_{i=0}^{n}\left(\boldsymbol{d}_{i\mathrm{I}}\boldsymbol{n}_{\mathrm{I}}\boldsymbol{F}_{i\mathrm{I}} + \boldsymbol{d}_{i\mathrm{II}}\boldsymbol{n}_{\mathrm{II}}\boldsymbol{F}_{i\mathrm{II}}\right) \\ S.t: d_j > 0\left(d_j = 0\right) \| F_j = 0\left(F_j > 0\right), s_z \geq 0, F_j \geq 0 \end{cases}, \tag{30}$$

where $\boldsymbol{P}$ is the tooth surface load, and $\boldsymbol{P} = [\boldsymbol{F}_{\mathrm{I}}; \boldsymbol{F}_{\mathrm{II}}]$; $j = 1,2,3,\cdots,2n$; I,II represent the first and the second pair of teeth; $[S]$ is the flexibility matrix of the tooth contact point; $\boldsymbol{S} = \begin{bmatrix}\boldsymbol{S}_{\mathrm{I}} & 0; 0 & \boldsymbol{S}_{\mathrm{II}}\end{bmatrix}$; $[F]$ is the load matrix of the tooth contact point; $[w]$ is the initial clearance matrix; $[d]$ is the residual clearance matrix; $\boldsymbol{n}_{\mathrm{I}}$ and $\boldsymbol{n}_{\mathrm{II}}$ are the unit normal vectors of the first and the second pair of teeth; $\boldsymbol{d}_{i\mathrm{I}}$ and $\boldsymbol{d}_{i\mathrm{II}}$ are the matrixes composed of the rotation radius of discrete points on the contact line; $[e]$ is the unit diagonal matrix; s_z is the normal displacement of the gears driven under external load.

Fig. 20 shows the influence of the cutter errors on the tooth surface load distribution. Fig. 20 (a) shows the tooth surface load distribution of an ideal gear pair; Figs. 20 (b), (c), (d), (e) and (f) show the tooth surface load distribution of Δy=0.5 mm, γ=0.0052 rad, $\Delta\alpha$=0.2°, ΔR_{T}=5 mm, Δz=0.5 mm, respectively. Because Δz and β have the same impact on the load distribution, only the influence of Δz is discussed. It can be seen from Fig. 20 that the load distribution of the ideal gear is in the middle of the tooth width; the load distribution area deviates from the cross-section of the tooth width, when there are errors Δy and γ, load changes are reduced or increased; the load distribution position remains unchanged, when there is a tooth line radius error Δz, ΔR_{T} and $\Delta\alpha$. Observing the maximum load on the tooth surface, the tooth surface error increases when there is an error Δz; the tooth surface error decreases, when there is an error ΔR_{T}; $\Delta\alpha$ and γ errors have a certain influence on the load on the double-tooth meshing area.

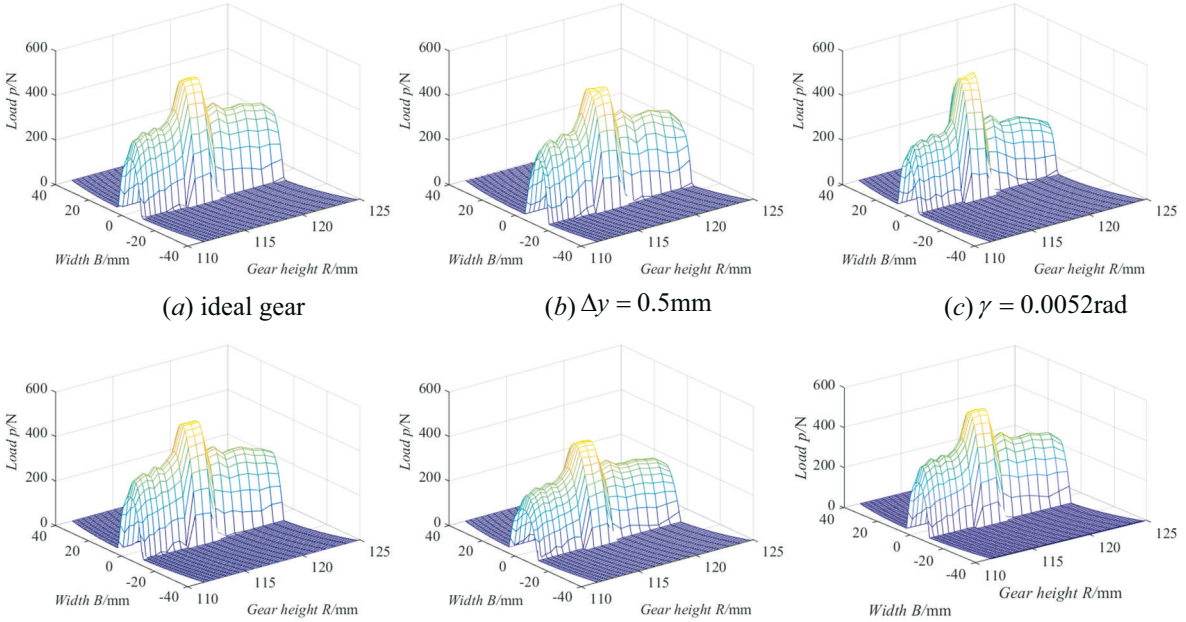

(*a*) ideal gear (*b*) $\Delta y = 0.5$mm (*c*) $\gamma = 0.0052$rad

(*d*) $\Delta\alpha = 0.2°$ (*e*) $\Delta R_T = 5$mm (*f*) $\Delta z = 2$mm

Fig. 20 Influence of cutter errors on distribution of tooth surface load

7. Conclusion

This paper discusses the influence of cutter errors on forming accurate VH-CATT cylindrical gears. Firstly, sources of errors in the tooth forming accuracy were analysed. Next, an ideal tooth surface equation and tooth surface equations with cutter errors of the VH-CATT cylindrical gear were deduced. Then, the tooth thickness error of the gear is used to represent the gear forming accuracy. Finally, influences of the cutter errors on the tooth thickness error and the gear contact were investigated. The main conclusions can be expressed as follows:

(1) The sources of error in the gear forming accuracy mainly include the position errors γ, β, Δx, Δy, Δz and the geometric errors $\Delta\alpha$ and ΔR_T.

(2) The absolute value of the tooth thickness error increases with an increase in β, and the tooth thickness decreases when the error is caused by clockwise rotation and increases when the error is caused by counterclockwise rotation. The tooth thickness error of the face width middle section is zero, but the tooth thickness error of the other sections increases with an increase in γ. The error of translation along the x-axis Δx has no influence on the tooth thickness error. The tooth thickness error increases with an increase in Δy and Δz. Further, the tooth thickness error of the pitch circle is zero, the tooth thickness error from the tooth root to the pitch circle is positive, and the tooth thickness error from the pitch circle to the tooth top is negative, and the tooth shape becomes sharp. The larger the tooth line radius error is, the greater the absolute value of the tooth thickness error closer to the tooth top and the end face is. The end face near the tooth top becomes sharp when ΔR_T is less than 0; the tooth thickness of the end face near the tooth top increases when ΔR_T is greater than 0. In a word, all errors except Δx have a certain influence on the tooth thickness error.

(3) γ and Δy make the actual meshing point deviate from the middle section, the other error items do not change the actual meshing point position, and the contact point position will change to the tooth face width end face if ΔR_T is too large; all the cutter errors have an influence on the contact area, load distribution and the maximum load on the tooth surface.

(4) The main future work will focus on the analysis of the influence of errors on contact performance and modification of the design method.

Acknowledgement

This study was supported by Guizhou Provincial Science and Technology Projects (grant number Qiankehejichu-ZK[2021]yiban273), the Zunyi Normal University 2021 Rural Revitalization Project (Qiaojiaohe KY Zi [2012]017-5), and the Natural Science Foundation of Sichuan (grant number 2022NSFSC1975).

REFERENCES

[1] Ma D., Liu Y., Ye Z., et al. Analysis of the Tooth Surface Contact Area of a Circular-Arc-Tooth-Trace Cylindrical Gear under Load. Transactions of Famena 2021,45(1),79-94. https://doi.org/10.21278/TOF.451018220

[2] Wu Y., Hou L., Ma D., et al. Milling Machine Error Modelling and Analysis in the Machining of Circular-Arc-Tooth-Trace Cylindrical Gears. Transactions of Famena 2020, 44(4),13-29. https://doi.org/10.21278/TOF.444009419

[3] Zhang, Q., Hou, L., Tang, R. Method of Processing and an Analysis of Meshing and Contact of Circular Arc Tooth Trace Cylindrical Gears. Transactions of FAMENA 2016, 40(4), 11-24. https://doi.org/10.21278/TOF.40402

[4] Tseng J T, Tsay C B. Mathematical Model and Surface Deviation of Cylindrical Gears With Curvilinear Shaped Teeth Cut by a Hob Cutter. Journal of Mechanical Design 2004, 127(5),271-277. https://doi.org/10.1115/1.1876437

[5] Tseng R T , Tsay C B . Mathematical model and undercutting of cylindrical gears with curvilinear shaped teeth. Mechanism and Machine Theory 2001, 36(11), 1189-1202. https://doi.org/10.1016/S0094-114X(01)00049-0

[6] Zhao F., Hou L., Duan Y., et. al. Research on the forming theory analysis and digital model of circular arc gear shaped by rotary cutter. Journal of Sichuan University: Engineering Science Edition 2016,48(6), 119-125. DOI: 10.15961/j.jsuese.2016.06.017

[7] Song A., Wu W., Gao S., et al. The Ideal Geometry Parameters of Arch Cylindrical Gear and Its Process Method. Journal of Shanghai Jiaotong University 2010,44(12), 1735-1740.

[8] Ma Z., Deng C. CNC Machining Method of Whole Modified Surface of Cylindrical Gears with Arcuate Tooth Trace. Journal of Mechanical Engineering 2012,48(5), 165-171. https://doi.org/10.3901/JME.2012.05.165

[9] Zhenqun M., Yanjue G., Xiaochun W. Symmetric arcuate tooth trace clindrical gearing. Chinese Journal of Mechanical Engineering 2004, 17(DecS): 94-97. https://doi.org/10.3901/CJME.2004.supp.094

[10] Wang S., Hou L., Dong L. Modeling and strength analysis of cylindrical gears with curvilinear shape teeth for manufacture. Journal of Sichuan University 2012, 44 (2),210-215. DOI: 10.15961/j.jsuese.2012.02.029

[11] Ma D., Wei Y., Ye Z., et al. Mesh contact impact of circular arc tooth trace cylindrical gears. Journal of Vibration and Shock 2018,37(7): 123-131. DOI: 10.13465/j.cnki.jvs.2018.07.019

[12] Ma D. , Liu Y. , Ye Z. Meshing Contact Impact Properties of Circular Arc Tooth Trace Cylindrical Gear Based on Rotating Knife Dish Milling Process. Mathematical Problems in Engineering 2021,2021:1- 17. https://doi.org/10.1155/2021/8819818

[13] Sun Z., Hou L., Wang J. Contact strength analysis of circular-arc-tooth-trace-cylindrical gear. Journal of the Brazilian Society of Mechanical Sciences and Engineering 2016, 38(3): 999-1005. https://doi.org/10.1007/s40430-014-0272-6

[14] Wei Y., Guo R. , Liu Y. Analytical Calculation of the Tooth Surface Contact Stress of Cylindrical Gear with Variable Hyperbolic Circular Arc Tooth Trace. Symmetry 2020,12(8):1318. https://doi.org/10.3390/sym12081318

[15] Fuentes-Aznar,A.,Ruiz-Orzaez,R., Gonzalez-Perez, I. Comparison of spur, helical and curvilinear gear drives by means of stress and tooth contact analyses. Meccanica 2017, 52(7), 1721-1738. https://doi.org/10.1007/s11012-016-0515-y

[16] Fuentes, A., Ruiz-Orzaez, R., Gonzalez-Perez, I. Computerized design, simulation of meshing, and finite element analysis of two types of geometry of curvilinear cylindrical gears. Computer Methods in Applied Mechanics & Engineering 2014, 272 (2), 321-339. https://doi.org/10.1016/j.cma.2013.12.017

[17] Zhang X, Xie Y, Tan X. Design, meshing characteristics and stress analysis of cylindrical gears with curvilinear tooth profile. Transactions of Famena 2016,40 (1), 27-44.

[18] Zhang X., Liang Z. Comparison of Conventional Double-Helical and Curvilinear Cylindrical Gear Drives in Terms of Transmission Errors and Stress. Transactions of Famena 2021, 45(3),1-18. https://doi.org/10.21278/TOF.453016020

[19] Chen, Y. C., C. C. Lo. Contact stress and transmission errors under load of a modified curvilinear gear set based on finite element analysis. ARCHIVE Proceedings of the Institution of Mechanical Engineers Part C Journal of Mechanical Engineering Science 2015,203-210 (229.2),191-204. https://doi.org/10.1177/0954406214532907

[20] C Gosselin. Effects of the machine settings on the transmission error of spiral bevel gears cut by the Gleason method. American Society of Mechanical Engineers 1989 ,60(2):705-712.

[21] FL Litvin. Generated Spiral Bevel Gears: Optimal Machine-Tool Settings and Tooth Contact Analysis. NASA Technical Memorandum 1985,11(12):999-1005. https://doi.org/10.4271/851573

[22] Tang J., Lu Y., Zhou C.. Error Tooth Contact Analysis of Spiral Bevel Gears Transmission. Journal of Mechanical Engineering 2008, 44 (7): 16-23. DOI: 10.3321/j.issn:0577-6686.2008.07.003

[23] Tang J., Cao K., Li G., et al. Research on the Effect Law between Machine Setting Parameter Errors and Hypoid Gears Surface Errors. Journal of Mechanical Engineering 2010, 46(17):179 -185. https://doi.org/10.3901/JME.2010.17.179

[24] Zhou C., Tang J., Zeng T., et al. Relationship between Grinding Wheel and Tooth Surface Error. Journal of Mechanical Engineering 2008,44(2):100-107. DOI: 10.3321/j.issn:0577-6686.2008.02.016

[25] Litvin F. L. Gear geometry and applied theory. PTR Prentice Hall Press 1994.

[26] Ma, D. Q., Ye, Z. H., Yang, H. Tooth surface reconstruction and tooth profile geometric analysis of circular arc tooth trace cylindrical gears. Transactions of Famena 2019, 43(1),29-44. https://doi.org/10.21278/TOF.43103

[27] Simon V V. Multi-objective optimization of hypoid gears to improve operating characteristics. Mechanism and Machine Theory 2020, 146,103727. https://doi.org/10.1016/j.mechmachtheory.2019.103727

[28] He Z., Tang W., Sun S. A Model for Analysis of Time-Varying Mesh Stiffness of Helical Gears with Misalignment Errors. Transactions of Famena 2021, 45(2),59-73. https://doi.org/10.21278/TOF.452021720

Submitted: 07.7.2022

Accepted: 29.6.2023

Dengqiu Ma*
School of Engineering and Technology, Zunyi Normal College, Zunyi, China; School of Mechanical and Electrical Engineering, Lanzhou University of Technology Lanzhou, China

Yongping Liu
School of Mechanical and Electrical Engineering, Lanzhou University of Technolog, Lanzhou, China

Zhenhuan Ye
School of Engineering and Technology, Zunyi Normal College, Zunyi, China

Dawei Li
School of Mechanical and Electrical Engineering, Lanzhou University of Technolog, Lanzhou, China

Yang Wu
School of Mechanical Engineering, Sichuan University, Chengdu, China
*Corresponding author:
scumdq@163.com